Pressure-Mediated Structural Transitions in Nitrogen-Rich 1H-Tetrazole: New Insight from Dispersion Corrected Density Functional Theory Calculations

Wenpeng Wang[a,*], Qijun Liu [b] and Zhengtang Liu [c]

[a] *School of Science, Xi'an University of Posts and Telecommunications, Xi'an 710121, China*
[b] *School of Physical Science and Technology, Southwest Jiaotong University, Chengdu 610031, China*
[c] *State Key Laboratory of Solidification Processing, Northwestern Polytechnical University, Xi'an 710072, China*

Received: 05.04.2022 & Accepted: 13.06.2022

Doi: 10.12693/APhysPolA.142.285 *e-mail: wangwenpeng@xupt.edu.cn

Heterocyclic nitrogen-rich molecules are widely used as effective precursors for the preparation of high energy density materials, which are denser than their carbon analogs. Here, dispersion corrected density functional theory calculations have been used to study the effect of pressure on nitrogen-rich 1H-tetrazole. A good agreement was achieved between the calculated and experimental crystal structures under ambient conditions. Furthermore, the vibrational spectra were computed by the linear response method as implemented in density functional perturbation theory, and infrared vibrational modes were assigned. The anomaly changes with increasing pressure in the lattice parameters, bond angles, and band structure were observed, indicating that a pressure mediated structural transition occurred around 4 GPa. Subsequently, a mechanism was proposed from the behavior of the vibration spectrum, that is, the structural changes in the 1H-tetrazole molecules were related to the distortion of the ring and CH bond.

topics: high pressure, DFT, vibrational property

1. Introduction

In order to meet the growing military and civilian needs, nitrogen-rich compounds are currently the focus of most attention as potential high energy density materials (HEDMs) due to the large number of energetic N–N and/or N = N bonds [1]. At present, performing high-pressure on nitrogen-rich molecules is a favored approach for the synthesis of HEDMs [1, 2]. In particular, 1H-tetrazole is a promising nitrogen-rich molecule for the synthesis of polynitrogen materials [3]. 1H-tetrazole has a relatively simple molecular structure and possesses a high nitrogen content of 80%. Some experimental efforts and theoretical calculations were performed to understand its structural and vibrational properties at ambient conditions [4, 5].

Recently, Li et al. studied the high-pressure behavior of 1H-tetrazole by X-ray diffraction and Raman spectroscopy [6]. The authors found a crystalline-to-crystalline phase transition above 3 GPa and an amorphous phase transition around 14 GPa. The high-pressure phase possessed a P1 space group, and there were two non-equivalent molecules in the unit cell. Later, Gao et al. reported the pressure-induced phase transition and chemical reaction of 1H-tetrazole by Raman, infrared (IR), X-ray diffraction, and neutron diffraction [3]. In contrast to the results of Li et al. [6], although the authors found a phase transition around 3 GPa as well, the high-pressure phase only possessed one molecule in the unit cell. To verify this high-pressure structure of 1H-tetrazole, the authors further calculated the enthalpy values of their own experimental structure and those reported by Li et al. [6], and found that the enthalpy values of their reported structure were lower, indicating that their experimental structure was more reasonable. Similarly, Liu et al. studied the pressure-induced phase transition of 1H-tetrazole using Raman, IR, X-ray diffraction, and neutron diffraction [7]. They found a phase transition from the low-pressure to the high-pressure phase occurred around 4 GPa. The authors suggest that the high-pressure phase of 1H-tetrazole contained two non-equivalent molecules in the unit cell. Moreover, based on the Raman and IR data, another pressure-induced transition around 9 GPa was identified. The further

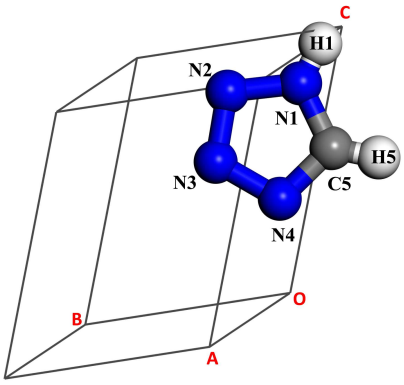

Fig. 1. Crystal structure of 1H-tetrazole.

calculated phonon density of states showed that the vibrational intensity and frequency of the nitrogen and hydrogen atoms presented nonlinear changes around 9 GPa, which the authors claim was due to the formation of new hydrogen bonds.

Here, we report a detailed study of high-pressure structural and vibrational behaviors of 1H-tetrazole because (i) the structural response of simple molecular solids under high pressure is one of the basic problems in condensed matter physics and solid-state chemistry, and studying the high-pressure structure behavior of 1H-tetrazole can help us understand the high-pressure synthesis of HEDMs, (ii) although the structure of 1H-tetrazole has been studied experimentally, its high-pressure structural behavior is still controversial, and there is still a lack of theoretical studies on the microstructural responses. To address these two objectives, density functional theory (DFT) calculations were conducted to simulate 1H-tetrazole crystal and molecular structures and electronic properties, and the density functional perturbation theory (DFPT) approach was employed to compute IR spectra compression up to 10 GPa. The theoretical methods used in this work are described next.

2. Theoretical methods

The density functional theory calculations were performed using the Cambridge Sequential Total Energy Package (CASTEP) packages [8]. The crystal structure of 1H-tetrazole [9] was adopted in our starting calculations. In the geometry optimization, the total energy was converged less than 5×10^{-6} eV/atom, the residual bulk stress less than 0.02 GPa, the residual force less than 0.01 eV/Å, and the displacement of atoms less than 5×10^{-4} Å. The norm-conserving pseudopotentials [10] were used with a 990 eV cutoff. Integrations in the Brillouin zone of the reciprocal space were sampled with a $7 \times 6 \times 6$ Monkhorst–Pack grid (126 k-points used) [11]. The structural parameters were optimized by the Broyden–Fletcher–Goldfarb–Shanno (BFGS) method [12]. The generalized gradient approximation (GGA) with the Perdew–Burke–Ernzerhof (PBE) parameterization [13] was used. Tkatchenko–Scheffler (TS) method was used in order to include the long-range intermolecular interactions [14]. After the structure optimization, the vibrational spectrum was simulated by using the linear response method as implemented in density functional perturbation theory [15].

3. Results and discussion

The crystal structure of 1H-tetrazole has been reported [9] to possess a triclinic unit cell, a =3.725 Å, $b = 4.773$ Å, $c = 4.936$ Å, $\alpha = 107.03°$, $\beta = 107.23°$, $\gamma = 101.57°$, as shown in Fig. 1. The calculated lattice parameters of 1H-tetrazole in the company of experimental data are shown in Table I. In general, the calculated lattice parameters are well-reproduced experiments. The calculated a, b, and c are 3.674, 4.786, and 4.925 Å, which were only overestimated/underestimated by −1.4, 0.3, and −0.2%, respectively. Our calculated crystal angles α, β, γ, and unit cell volume V are also satisfactory, with calculated errors of 0.1, 0.1, −1.3, and -0.6%, respectively. Although comparisons of lattice parameters between the calculated and experimental crystal structures are helpful in understanding whether the calculated structures have realistic distances between the molecules, it is also important to evaluate whether the simulated intermolecular close contacts are similar to those that exist in the experimental structures [16]. Hirshfeld surfaces provide a quantitative measure of intermolecular contacts by sampling the electron density around each molecule and correlating the close molecular contact that occurs at the surface to a particular atomic type (detailed descriptions can be found elsewhere [17–20]). Table II shows the various intermolecular close contacts of 1H-tetrazole, demonstrating that the calculated structures are matched well with the experiment. It can be seen from the above results that dispersion corrected DFT (DFT-D) and the PBE+TS functional approach employed here can provide reasonable values.

TABLE I

The lattice parameters of 1H-tetrazole at ambient condition. The values in parentheses are the percentage error deviations from experimental data.

	This work	Experimental [9]
a [Å]	3.674 (−1.4%)	3.725
b [Å]	4.786 (0.3%)	4.773
c [Å]	4.925 (−0.2%)	4.936
α [deg]	107.10 (0.1%)	107.03
β [deg]	107.32 (0.1%)	107.23
γ [deg]	100.23 (−1.3%)	101.57
V [Å^3]	75.61 (−0.6%)	76.09

TABLE II

Intermolecular close contact interactions as calculated from Hirshfeld surfaces.

	This work	Experimental [9]
C...C	0.1%	0.1%
C...N	5.6%	5.6%
C...H	2.5%	2.6%
N...N	10.0%	11.0%
N...H	79.2%	78.0%
H...H	2.6%	2.7%
C...C	0.1%	0.1%

The pressure dependence of the lattice parameters of 1H-tetrazole is shown in Fig. 2. Although the a, b, and c axes all shrunk with the increased pressure of up to 10 GPa, the a-axis is showing the maximum compression. For instance, the a-axis is 3.674 Å at ambient conditions, and when the pressure goes up to 10 GPa, its value is found to be 3.148 Å within the compressibility of 14.3%. In particular, the lattice angles α and β presented a discontinuous jump around 4 GPa, indicating a possible structural modification. The unit cell volume versus pressure curve can be fitted to the Birch–Murnaghan equation of state (BM-EOS) [21] as follows

$$P = \frac{3B_0}{2}\left[\left(\frac{V_0}{V}\right)^{\frac{7}{3}} - \left(\frac{V_0}{V}\right)^{\frac{5}{3}}\right] \times \left[1 + \frac{3}{4}(B' - 4)\left(\left(\frac{V_0}{V}\right)^{\frac{2}{3}} - 1\right)\right]. \quad (1)$$

The fitted EOS parameters are the unit cell volume at ambient condition $V_0 = 75.5$ Å^3, isothermal bulk modulus $B_0 = 13.7$ GPa, and its first derivative $B' = 6.3$. These values are consistent with the experimental values [3] $V_0 = 75.6$ Å^3, $B_0 = 13.6$ GPa, and $B' = 4$, respectively.

A detailed analysis of the effect of pressure on the calculated bond lengths is plotted in Fig. 3. It can be seen that the bond lengths in the heterocyclic ring of N1–N2, N2–N3, N3–N4, N4–C5, and C5–N1 all monotonously decrease with the pressure, whereas the bond lengths out of the heterocyclic ring of N1–H1 increase with the pressure. Figure 4 shows the effect of pressure on selected bond angles. Interestingly, there is a distinct discontinuous change around 4 GPa. Specifically, the bond angles of N4C5N1 first increase with increasing pressure, and then suddenly decrease after 4 GPa (see Fig. 4c). Similarly, the bond angles of H1N1C5 first increase and then cease with increasing pressure (Fig. 4d). These subtle changes are evidence of structural modifications [22, 23].

In order to understand the nature of structural changes, we further calculated the energy band of 1H-tetrazole using PBE-GGA+TS functionals,

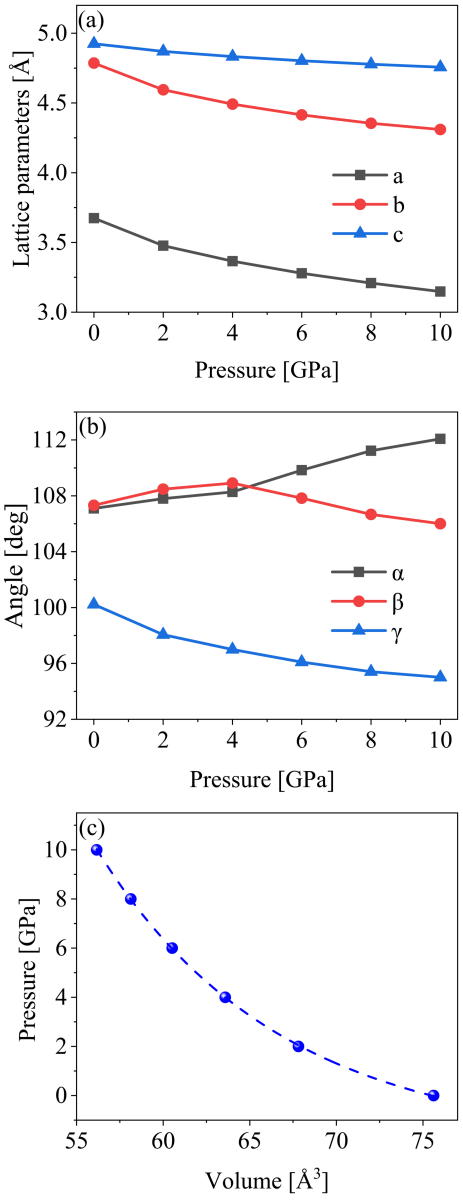

Fig. 2. Lattice parameter in 1H-tetrazole crystals as a function of pressure.

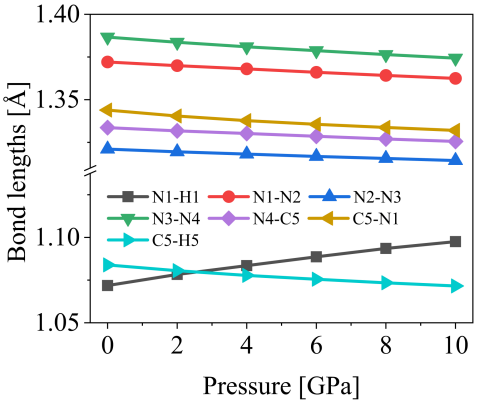

Fig. 3. Bond length in 1H-tetrazole as a function of pressure.

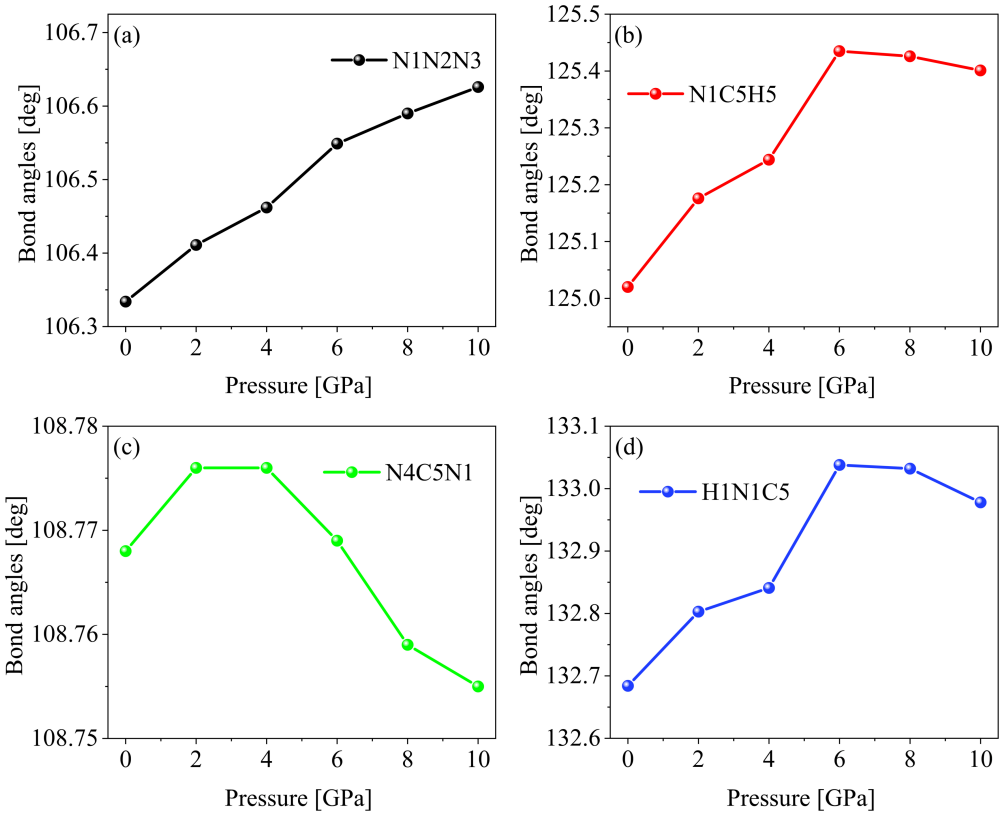

Fig. 4. Bond angle in 1H-tetrazole as a function of pressure.

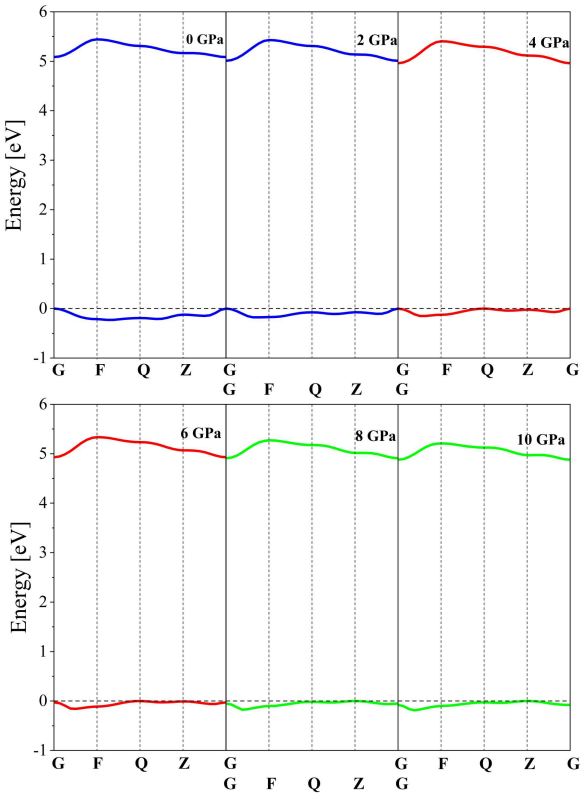

Fig. 5. The band structure of 1H-tetrazole under pressure.

as shown in Fig. 5. It was found that the bottom of the conduction band and the top of the valence band are along the *G*-point in the range of 0–2 GPa. Therefore, the 1H-tetrazole is a direct band gap. However, as the pressure continues to increase, at the top of the valence band at the *Q*-point, the 1H-tetrazole becomes an indirect band gap when the pressure goes up to 4 GPa. Subsequently, although 1H-tetrazole maintains its indirect band gap, the top of the valence band further becomes the Z-point as the pressure exceeded 6 GPa. It is suggested that the fact that such changes occur at the same pressures as pressure-related changes in lattice angles, bond distances, and electronic band structures is not just a coincidence, but evidence that a structural change has occurred.

Vibrational spectroscopy is an important tool for detecting molecular structural variations [24–28]. To further understand the molecular structure of 1H-tetrazole under high pressure, the IR spectra were simulated by the density functional perturbation theory. 1H-tetrazole crystallizes in the triclinic structure with space group P1. There are 7 atoms in the unit cell of 1H-tetrazole, the corresponding number of vibrational modes is 21, three of which are acoustic modes, and the other 18 are optical modes. Figures 6 and 7 show the calculated IR spectra and frequency shift under pressure, respectively. The vibrational modes in the low-frequency range (0–200 cm^{-1}) are assigned to the lattice mode

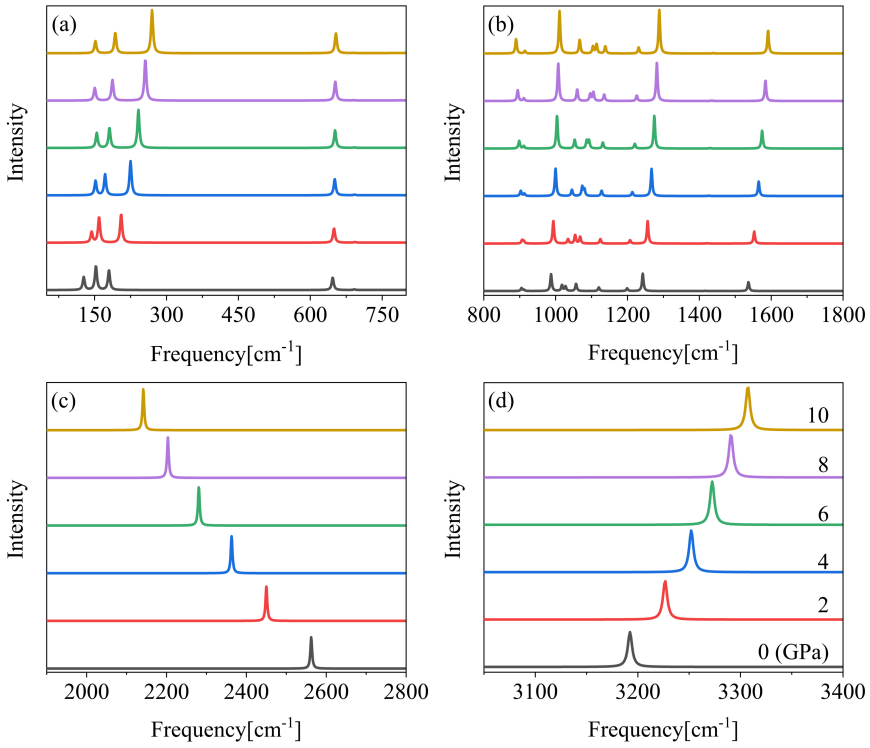

Fig. 6. The calculated IR spectra of 1H-tetrazole under pressure.

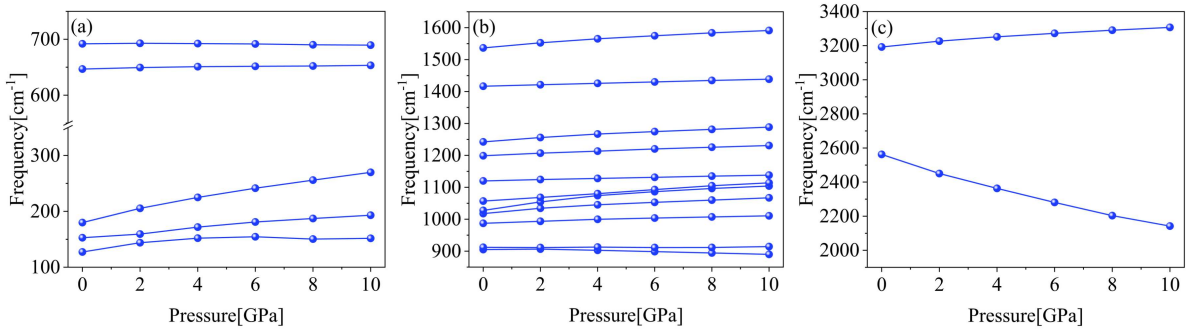

Fig. 7. IR frequency shifts of 1H-tetrazole as a function of pressure.

frequencies. It has been found that the lattice modes at 153 and 180 cm^{-1} shift towards high frequencies as the pressure increases. But the mode at 127 cm^{-1} presented an anomaly behavior; namely, the mode first increases with increasing pressure and then decreases around 6 GPa. The internal modes from 600 to 1600 cm^{-1} correspond to out-of-plane bending of the ring, in-plane bending of the ring, CH bending, NH bending, and ring stretching. The modes between 2500 and 3200 cm^{-1} correspond to NH stretching and CH stretching. It is clear that, with the exception of modes at 692, 905, and 2562 cm^{-1}, all internal modes from 600 to 3200 cm^{-1} shift towards higher frequencies with increasing pressure, which is consistent with the result that pressure leads to the increase of intermolecular repulsion force.

In the crystal of 1H-tetrazoles, the individual molecules are linked by N–H...N and C–H...N hydrogen bonding to form a two-dimensional network [9]. Based on the theory of hydrogen bonds segmented cooperative relaxation [29], for hydrogen bonding (D–H...A), when the distance of H...A is compressed, the Coulombic repulsion between D–A increases, which repels the D atom of the D–H bond and further promotes the elongation of the D–H covalent bond. As observed, the N–H stretching mode (2500 cm^{-1}) shows a redshift with increasing pressure, confirming the strengthening of the N–H...N hydrogen bonding, which can also be evidenced by the aforementioned results of the length of the N–H bond changing with pressure. Apart from this, the modes at 692 and 905 cm^{-1} are assigned to out-of-plane bending of the ring and CH bending,

respectively. With the increase of pressure in both modes, first a blueshift appears, and then, after 4 GPa, a redshift, indicating that the structural changes may be related to the distortion of the ring and CH bond.

4. Conclusions

In this work, the effects of pressure on the structural and vibrational properties of nitrogen-rich 1H-tetrazole were investigated by the dispersion corrected density functional theory (DFT-D) calculations. From the calculated crystal parameters and molecular geometry, the PBE+TS functional approach can provide reasonable values. It was found that the pressure dependence of the unit cell constants showed an anisotropic behavior, where a-axis has greater compression than the other two axes. Furthermore, the calculated bulk modulus $B_0 = 13.7$ GPa and its first derivative $B' = 6.3$ were in good agreement with experimental data. The lattice parameters, bond angles, and electronic band structures showed an anomaly change around 4 GPa, indicating the existence of a structural transition. In addition, the IR vibrational spectrum was calculated using the linear response method, and the vibrational modes and their dependence on pressure were determined. On the basis of the molecular geometry and vibrational modes results, a possible mechanism is proposed in an attempt to explain the pressure-induced structural transition. It was suggested that the structural modifications were associated with the distortion of the ring and CH bond in 1H-tetrazole.

Acknowledgments

This work was supported by the National Natural Science Foundation of China (Grant No. 12104364).

References

[1] M. Bykov, E. Bykova, G. Aprilis et al., *Nat. Commun.* **9**, 1 (2018).

[2] R. Turnbull, M. Hanfland, J. Binns, M. Martinez-Canales, M. Frost, M. Marqués, R.T. Howie, E. Gregoryanz, *Nat. Commun.* **9**, 4717 (2018).

[3] D. Gao, X. Tang, X. Wang et al., *Phys. Chem. Chem. Phys.* **23**, 19503 (2021).

[4] F. Billes, H. Endrédi, G. Keresztury, *J. Mol. Struct. THEOCHEM* **530**, 183 (2000).

[5] S.C.S. Bugalho, A.C. Serra, L. Lapinski, M.L.S. Cristiano, R. Fausto, *Phys. Chem. Chem. Phys.* **4**, 1725 (2002).

[6] W. Li, X. Huang, K. Bao et al., *Sci. Rep.* **7**, 1 (2017).

[7] Y. Liu, H. Du, L. Fang, F. Sun, H. Su, Z. Ge, W. Guo, J. Zhu, *RSC Adv.* **11**, 21507 (2021).

[8] M.D. Segall, P.J.D. Lindan, M.J. Probert, C.J. Pickard, P.J. Hasnip, S.J. Clark, M.C. Payne, *J. Phys. Condens. Matter* **14**, 2717 (2002).

[9] R. Goddard, O. Heinemann, C. Krüger, *Acta Crystallogr. Sect. C Cryst. Struct. Commun.* **53**, 590 (1997).

[10] D.R. Hamann, M. Schlüter, C. Chiang, *Phys. Rev. Lett.* **43**, 1494 (1979).

[11] H.J. Monkhorst, J.D. Pack, *Phys. Rev. B* **13**, 5188 (1976).

[12] T.H. Fischer, J. Almlöf, *J. Phys. Chem.* **96**, 9768 (1992).

[13] J.P. Perdew, K. Burke, M. Ernzerhof, *Phys. Rev. Lett.* **77**, 3865 (1996).

[14] A. Tkatchenko M. Scheffler, *Phys. Rev. Lett.* **102**, 6 (2009).

[15] S. Baroni, S. de Gironcoli, A. Dal Corso, P. Giannozzi, *Rev. Mod. Phys.* **73**, 515 (2001).

[16] B. Schatschneider, S. Monaco, A. Tkatchenko, J. Liang, *J. Phys. Chem. A* **117**, 8323 (2013).

[17] M.A. Spackman, D. Jayatilaka, *Cryst. Eng. Comm.* **11**, 19 (2009).

[18] S. Li, R. Bu, R.J. Gou, C. Zhang, *Cryst. Growth Des.* **21**, 6619 (2021).

[19] H. Shelton, P. Dera, S. Tkachev, *Crystals* **8**, 1 (2018).

[20] S.R. Madsen, J. Overgaard, D. Stalke, B.B. Iversen, *Dalt. Trans.* **44**, 9038 (2015).

[21] F. Birch, *J. Appl. Phys.* **9**, 279 (1938).

[22] A. Liang, C. Popescu, F.J. Manjon, P. Rodriguez-Hernandez, A. Muñoz, Z. Hebboul, D. Errandonea, *Phys. Rev. B* **103**, 054102 (2021).

[23] A. Liang, S. Rahman, P. Rodriguez-Hernandez, A. Muñoz, F.J. Manjón, G. Nenert, D. Errandonea, *J. Phys. Chem. C* **124**, 21329 (2020).

[24] B.B. Averkiev, Z.A. Dreger, S. Chaudhuri, *J. Phys. Chem. A* **118**, 10002 (2014).

[25] S. Appalakondaiah, G. Vaitheeswaran, S. Lebčgue, *J. Chem. Phys.* **138**, 184705 (2013).

[26] W.G. Li, Y.D. Gan, Z.X. Bai et al., *Phys. Chem. Chem. Phys.* **24**, 4462 (2022).

[27] S. Mondal, G. Vaitheeswaran, M.K. Gupta, R. Mittal, *J. Phys. Condens. Matter* **32**, 425502 (2020).

[28] N. Yedukondalu, V.D. Ghule, G. Vaitheeswaran, *J. Chem. Phys.* **145**, 064706 (2016).

[29] Y. Huang, X. Zhang, Z. Ma, Y. Zhou, W. Zheng, J. Zhou, C.Q. Sun, *Coord. Chem. Rev.* **285**, 109 (2015).